Available online at www.sciencedirect.com

ScienceDirect

Materials Today: ProceedingsXX (2016) XXX–XXX

materialstoday: PROCEEDINGS

www.materialstoday.com/proceedings

PMME 2016

Feature Fusion for FDG-PET and MRI for Automated Extra Skeletal Bone Sarcoma Classification

K. Baskaran[a] and R. Malathi[b]*

[a] Assistant Prof., Department of ECE,Dr PEC/ [*]Research Scholar Department EIE, Annamalai University, Tamil Nadu, India
[b*]Professor, Department of EIE, Annamalai University, Chidambaram, Tamil Nadu India

Abstract

The aim of the current work is the evaluation of Positron Emission Tomography (PET) utilizing 18F-Fluoro-2-Deoxy-Dglucose (FDG) when compared to volumetric as well as standard Magnetic Resonance Imaging (MRI) variables for assessing histological responses in bone sarcoma afflicted individuals. The generation of novel composite texture from combining FDG-PET as well as MRI data is examined to see if aggressive tumors could be better identified. For this particular objective, retrospective evaluation was performed on a group of 51 individuals in the same age group. All the patients had pre-treatment FDG-PET as well as MRIs consisting of T1-weighted as well asT2-weighted Fat-Suppression Sequences (T2FS). 9 non-textural features (SUV measures as well as shape attributes) as well as 41 textural features were extracted from the tumor area of distinct as well as fused scans. Extracting features was carried out by Grey Level Co-occurrence Matrix (GLCM), wavelet features. Selection of features was carried out by Correlation based Feature Selection (CFS) as well as Particle Swarm Optimization (PSO) and the classification was done by K-Nearest Neighbor (KNN), J48 as well as Neural Network (NN).From the simulations, it is found that the suggested method attained best classification accuracy.

Selection and Peer-review under responsibility of International Conference on Processing of Materials, Minerals and Energy (July 29th – 30th) 2016, Ongole, Andhra Pradesh, India.

*Keywords:*Bone Sarcoma; Magnetic Resonance Imaging (MRI); FluorDeoxyGlucose - Positron Emission Tomography (FDG-PET); Grey Level Co-occurrence Matrix (GLCM); Wavelet; Correlation based Feature Selection (CFS); Particle Swarm Optimization (PSO); Classifiers.

* Corresponding author. Tel.: +91 9443879055;
*E-mail address:*vsmalu@gmail.com

Selection and Peer-review under responsibility of International Conference on Processing of Materials, Minerals and Energy (July 29th – 30th) 2016, Ongole, Andhra Pradesh, India.

1. Introduction

Sarcomas refer to malignant tumors with mesenchymal origins which emerge in connective tissue, as opposed to the more common as well as well-known carcinomas that have epithelial origins. Sarcomas are very diverse and comprise greater than seventy histological sub-kinds as well as a rising quantity of molecular sub-kinds. They can grow at any time from childhood and appear anywhere on the body with differing aggressiveness, even if they are of the same histological sub-kind. Three major types of sarcomas are present which relate to varying clinico-pathological entities with particular progressions ad especially various management schemes: bone sarcomas, visceral sarcomas which grow in a particular organ as well as Soft Tissue Sarcomas (STS) that arise in connective as well as extra—osseous connective tissue. All these comprise around one percent of all adult carcinomas [1].

Bone comprises cartilaginous, osteoid, fibrous tissue as well as bone marrow elements. All tissues are capable of giving rise to benign or even malignant spindle cell tumor. Bone tumors may be sorted based on cell kind or recognized products of proliferating cells. All tumors are regarded as distinct clinico-pathological entities. Radio graphical, histological as well as clinical data are required for forming accurate diagnoses as well as for determination of the degree of activity as well as malignancy of all lesions.

Spindle cell sarcomas of the bone consist of diagnostically heterogeneous groups of malignant tumors such as Fibro-Sarcoma (FS), Malignant Fibrous Histiocytoma (MFH), leiomyosarcoma as well as non-differentiated sarcomas. They are present in age groups which also give rise to chondrosarcoma yet the skeletal distribution is almost identical to osteosarcoma. It is generally accompanied with pain as well as possibilities of fractures at presentation. Men are more vulnerable to it than women [2].

Neoadjuvant chemotherapy is effective in significantly improving survival rate but efficacy of chemotherapies may be dependably measured solely after tumor resections as well as histo pathological examinations. Apart from tumor volume as well as tumor resections, tumor regressions after neoadjuvant polychemo therapies are a significant prognostic element in pediatric sarcomas as per Salzer-Kuntschik.

Apart from histological response assessments, diagnostic imaging presents a way for monitoring therapy-associated impacts on the tumor post neoadjuvant treatments. Another benefit of response assessments by diagnostic imaging is earlier response assessments that ensure risk-adapted pre-operative chemotherapy with truncated non-effective neoadjuvant therapy or even intensifying effective pre-operative treatments. Moreover, earlier response assessments through diagnostic imaging allows for earlier identification of optimum surgical methods [3].

Imaging is a crucial technology in medical sciences for visualization of anatomical structure of the human body. Many novel complex medical imaging methods like X-ray, MRI and ultrasound all rely greatly on computerized technology for generating or displaying digitized images. MRI is an advanced method utilized for medical imaging as well as for studying the several states of the human brain. MRIs offer plenty of data regarding the brain that may be utilized for studying, diagnosing as well as for carrying out clinical analyses of the brain for figuring out if it is normal or anomalous. But the data extricated from the images is a lot and it is difficult to reach conclusions on a diagnosis on the basis of raw information. In those cases, it is necessary to utilize several image analysing tools for examining the MRIs and extracting conclusive data for classifying brain as either normal or anomalous.

MRIs are typically the technique chosen for medical images when soft tissue delineation is required. This is particularly true for attempts to sort brain tissue. The primary benefit of MRI is that it is a non-invasive method. The usage of computerized technology in supporting medical decisions is vast and is pervading several domains. Completely automated normal as well as anomalous brain classifications from MRIs are considerably important for research as well as clinical study.

Identifying brain structures in MRIs is significant in neurons scientific studies and has several applications like mapping functional activations in brain anatomies, studying brain development as well as analyzing neuro anatomical variabilities in normal brains. Brain image segmentations are helpful in clinically diagnosing neurodegenerative as well as psychiatric disorders, treatment evaluations, as well as surgical planning. Several techniques are present for automated as well as semi-automated image segmentation although almost all of them experience failures due to unknown noises, bad image contrasts as well as weak boundaries typical in medical images [4].

MRI is a typical way for visualizing brain structures. On the basis of the imaging method, studying primary cerebral tissue is particularly a significant point within the context of CAD as well as patient follow-ups. These

studies typically require an initial segmentation stage that focuses on splitting intracranial volume into possibly overlapping components: WM, GM, as well as Cerebro-Spinal Fluid (CSF). When handling MRI brain information, principal issue associated with segmentations is dealing with the following image decomposition elements: 1) acquisition noise, 2) Partial Volume Effect (PVE) as well as 3) bias field.

Fluorine 18 FDG-PET has been revealed as helpful in detecting nodal as well as distant metastases in individuals with soft tissues sarcoma. But, in spite of the rising usage of FDG PET/CT in managing bone as well as soft tissue sarcoma, no studies till data have compared the diagnostic accuracies of pre-operative staging with PET/CT, PET, as well as conventional imaging, as far as is known.

Features extraction refers to the procedure of creating features for usage in selection as well as classification jobs. Features selection has an important part to play in several patterns recognition issues like the classification of images. Although several attributes may be used for characterizing images, merely small quantities of them are effective in classifications. Greater number of features does not promise better classification performance, and so features selection is typically carried out for selecting compact as well as relevant features subset for reducing dimensionality of features space, which gradually enhances classification accuracy and decreases time consumptions [5].

The significance of features selection techniques is the selection of useful genes before classifying microarray data for predicting as well as diagnosing cancers. Features selection discards non-relevant as well as repetitive features for improving classification accuracy. Features selection techniques may either be filter or wrapper and embedded or hybrid. Filters choose features with no intervention by data mining algorithms. They are tested on the basis of 4 evaluatory criteria which are distance, information, dependency as well as consistency. Wrappers choose features subset on the basis of classifiers and rank features subsets through predictive accuracy or cluster excellence. They are also computationally more costly than filters.

At the time of extracting or selecting features, technique of potential subsets obtained by several variable settings in the event of features extraction or with regard to choosing the best feature extricated. Total searches are NP-hard issues, because searches become computationally intractable when search area widens. EA as well as SI protocols are utilized for solving NP-hard issues. The latter owe their inspiration to biological or natural phenomena wherein group intelligence arises from a set of small agents. The agents sense, interact as well as alter their environment in a local fashion. Almost all work in literature revolves around the issue of selecting features, but there is not enough work on variable optimization in the features extraction phase itself such that ideal features are extricated thereby reducing dimensionality of features set.

This study evaluates Fuzzy Bee segmentation for medical image processing. Two classifiers are used for medical images classification. The remaining part of the investigation is structured thus. Section 2 explains various methods used in the study. Section 3reveals experimental results while Section 4provides the conclusion for the study.

2. Methodology

In this section, GLCM and wavelet based feature extraction methods, CFS and PSO based feature selection techniques and KNN, J48 and NNs based classifiers are described.

2.1. Dataset

Patient Cohort: After the approval of the Research Ethics Board (REB), a dataset of 51 patients with histologically proven primary Soft-Tissue Sarcoma (STSs) of the extremities (represented as STS) was acquired in a retrospective manner. The patients were split into two: 1) 32 who did not develop lung metastases and 2) 19 who developed lung metastases at the time of the follow-up period. Those from the first group with follow-up time period lesser than a year were also removed from the research. Lung metastases were confirmed by biopsies or diagnoses by expert physicians from the presence of usual pulmonary lesions in CT/FDG-PET scans. Table 1gives summarized features of the dataset [6].

Table 1 Characteristics of STS Patient Cohort.

Characteristic	Type	No. of patients (%), n=51
Sex	Male	24 (47)
	Female	27 (53)
Age (y)	Range	16-83
	Mean ± STD	55 ± 17
Histology	Liposarcoma	11 (21)
	Malignant fibrous histiocytomas	17 (33)
	Leiomyosarcoma	10 (20)
	Synovial sarcoma	5 (10)
	Fibrosarcoma	1 (2)
	Extra skeletal bone sarcoma	4 (8)
	Other	3 (6)
Extremity site	Lower	47 (92)
	Upper	4 (8)
Grade	High	28 (55)
	Intermediate	15 (29)
	Low	5 (10)
	Upgraded	3 (6)
Recurrence/Spread	Distant–Lungs	19 (37)
	Distant-Other than Lungs	6 (12)
	Locoregional	4 (8)
	None	24 (47)
Treatment	Radiotherapy + Surgery	30 (59)
	Surgery + Chemotherapy	7 (14)
	Radiotherapy + Surgery + Chemotherapy	14 (27)

Imaging Data:

The 51 individuals obtained pre-treatment FDG-PET/CT as well as MRIs between November 2004 and 2011. For the PET part, a median of 420 of FDG was injected intravenously. Aroundsixty minutes after the injection, entire body two dimensional imaging acquisitions was carried out through various bed positions with median of 180s per bed position. PET attenuation corrected scans were recreated through usage of an Ordered Subset Expectation Maximization (OSEM) iterative protocol. MRI scans were the result of clinical acquisition with non-uniform protocol across patients.

Three kinds of MRI sequences generally utilized in clinical algorithms were chosen for research, which were the T1-weighted (T1), T2-weighted fat-saturated as well as Short Tau Inversion Recovery (STIR) sequences.

T1 sequences were obtained in axial plane for every patient. But individuals were scanned in varying planes with both or one of T2-weighted fat-saturated as well as STIR sequences that (macroscopically speaking) are both T2-weighted sequences which aim to suppress fat signals in the body (also known as T2FS). From a textural point of view, T2-weighted fat-saturated as well as STIR images are regarded as identical and so grouped in one scan category with merely one of the two sequences utilized per individual. T2-weighted fat-saturated scans were chosen default, because of their higher axial scan availability (n = 26). When T2-weighted fat-saturated scans were not present, STIR scans were utilized (n = 25).

2.2. Grey Level Co-occurrence Matrix (GLCM) Feature Extraction

Haralick et al. suggested Grey Level Co-occurrence Matrix representation of textural features for mathematical representation of grey level spatial dependence on textures in images. In this technique, co-occurrence matrices are created on the basis of orientation as well as distance between image pixels. Because fundamental textural patterns are governed by periodic occurrences of particular grey levels; co-occurrences of grey levels at pre-specified relative positions is an adequate metric of the presence of textures as well as periodicity of patterns [7].

It is a statistical method of identification of occurrences of grey level values in images as well as the identification of how all pixels are associated with adjacent pixels. GLCM, C, is expressed with regard to specified displacement h. While element (i , j), represented as c_{ij} , refers to the quantity of times a point possessing grey level j appears in position h relative to a point possessinggrey level i. If Nh is the quantity of pairs, then $C_{ij} = c_{ij} / Nh$ refers to the components of normalized C.

Probability metric may be expressed as:

$$P_r(x) = \{C_{ij} \mid \delta, e \mid\}$$

Wherein C_{ij} is given by:

$$C_{ij} = \frac{P_{ij}}{\sum_{i,j=1}^{G} P_{ij}}$$

Wherein P_{ij} denotes the quantity of occurrences of grey levels i as well as j, in a specified window as well as particular (δ-inter pixel distance, θ-orientation) pair. G refers to the quantized number of grey levels. Textural calculations lead to one number denoting the whole window. The number is placed in the position of center pixel of the window and window is shifted by one pixel and this procedure is iterated. In this manner, the whole image is created of textural values.

2.3. Wavelet Feature Extraction

Wavelets are a powerful mathematical tool for extracting features and have been utilized here for extracting wavelet coefficients from MRIs. Wavelets are localized basis functions that are scaled as well as shifted variants of certain fixed mother wavelets. The primary benefit of wavelets is that they offer localized frequency data regarding functions of signals that are considerably helpful in classifications [8]

Continuous wavelet transform x (t) of relative to a particular wavelet $\psi(t)$ is given by

$$W_{\psi}(a,b) = \int_{-\infty}^{\infty} x(t)\psi_{a,b}(t)\,dt$$

Where in

$$\psi_{a,b}(t) = \frac{1}{\sqrt{a}}\psi\left(\frac{t-a}{b}\right)$$

Wavelet $\psi_{a,b}(t)$ is computed from the mother wavelet $\psi(t)$ through translations as well as dilations: a refers to the dilation factor and b refers to the translation factor, both of which are real as well as positive numbers. Many various types of wavelets are present that have become famous because of the developments in wavelet analyses.

The most significant wavelet is known as the Harr wavelet, and it is the most simple as well as favoured wavelet for several applications.

$W_{\psi}(a,b)$ The equation may be discretized through restraint of a as well as b to discrete lattice ($a = 2^b$ & $a > 0$) for giving discrete wavelet transforms (DWT), which is given by:

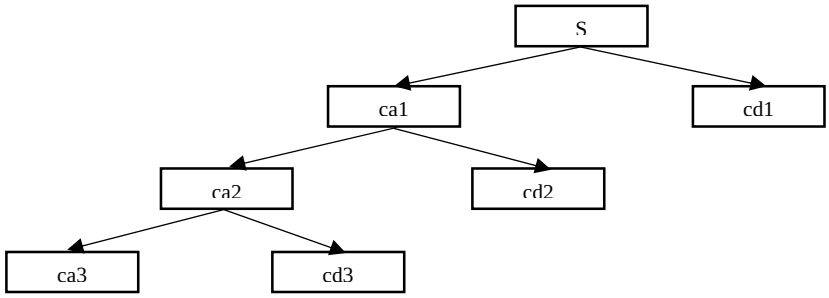

Fig. 1 3-level wavelet decomposition tree

$$ca_{j,k}(n) = DS\left[\sum_n x(n) g_j^*(n - 2^j k)\right]$$

$$cd_{j,k}(n) = DS\left[\sum_n x(n) h_j^*(n - 2^j k)\right]$$

Here $ca_{j,k}$ and $cd_{j,k}$ denote coefficients of approximation as well as detail elements correspondingly. g (n) as well as h(n) denote low-pass as well as high-pass filters correspondingly. j as well as k denote wavelet scale as well as translation element correspondingly. DS operators imply down sampling. The decomposition procedure is repeated with consecutive approximations being disintegrated in turns such that a single signal is decomposed into several levels of resolution. The entire procedure is known as wavelet decomposition tree, as given in Figure 1.

In the event of images, DWT is employed on every dimension in a separate fashion. Figure 2displays the schematics of 2D DWT.

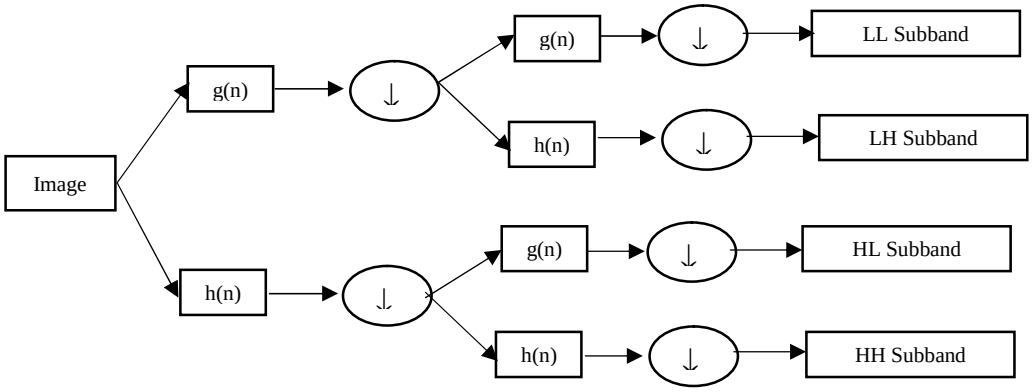

Fig. 2 Schematic diagram of 2D DWT

Consequently, there are four sub-bands (LL, LH, HH, as well as HL) images at every scale. LL is utilized for subsequent 2D DWT. LL sub-band is also considered as approximation part of the scan whereas LH, HL, HH sub-

bands are considered as the detailed parts of the scan. When level of disintegration is risen, more compact although more coarse approximation components are acquired. Hence, wavelets offer a basic hierarchical model for interpretation of image data. In the protocol, level-3 decomposition through Harr wavelet was used for extracting features.

2.4. Correlation based Feature Selection (CFS)

CFS may be executed through three heuristic search schemes which are the forward selection, backward elimination as well as the best first scheme. The first begins with an empty set of features and appends one feature at a time. This is iterated till no possible feature addition causes greater evaluation. With the case of backward elimination, complete set of features is initially present and one by one features are removed and this is continued so lond as heuristic evaluation is not degraded.

Best first scheme may have empty or full set of features initially. If it begins with empty set, forward selection is employed and if it begins with complete set, backward elimination is utilized. Best first scheme ends after a certain number of cycles or when particular criteria are fulfilled. CFS functions under the presumption that features are conditionally independent [9].

CFS protocol utilizes correlation based objective functions for evaluating the utility of the attributes. Objective functions $J_{cfs}(\lambda)$, additionally called Pearson's correlation coefficient, have their basis in the heuristic that excellent features subset has excellent correlation with class labels and yet maintain least correlation amongst themselves.

$$J_{cfs}(\lambda) = \frac{\lambda \psi_{cr}}{\sqrt{\lambda + \lambda(\lambda - 1)\psi_{rr}}}$$

The equation given previously shows the advantages of λ features subset wherein ψ_{cr} refers to the average feature-class correlation while ψ_{rr} refers to average feature-feature correlation in the class. CFS based features selection protocol utilizes $J_{cfs}(\lambda)$ for searching features subset through best first scheme. Best search begins with testing of all individual attributes by regarding them as distinct subsets.

2.5. Particle Swarm Optimization (PSO)s

PSO, presented by Kennedy and Eberhart, is one among a vast set of SI techniques. It was initially suggested as simulating social behavior and as an optimization technique. PSO is simple in concept and may be executed in very less number of lines of code. PSO individuals retain knowledge of its best performance position whereas in Genetic Algorithm, if individuals are not chosen for crossovers or mutations, data held onto by the individuals are discarded [10].

In PSO, swarms comprise individuals known as particles that alter their position $x_i(t)$ with time t. All particles represent possible solutions to issues and fly around in multi-dimensional search spaces. At the time of movement, all particles adjust their positions as per their experiences as well as based on collective experiences of neighboring particles, thereby exploiting best positions found by itself as well as the swarm. This leads to particles moving toward optimal solution. Performances of all particles are assessed as per pre-specified fitness functions that are related to the issue being resolved.

For implementing PSO, neighbor hoods in the related population are to be defined and then relationships between particles which are part of the neighbourhood are also to be described. In this particular context, several topologies like star, ring or wheel are present. Here, ring topology is utilized wherein all particles are related with two neighbours and attempt is made to mimic best neighbour by travelling close to optimal solution discovered within the neighbourhood.

2.6. K-Nearest Neighbour (KNN) Classifier

K-Nearest neighbour is a famous learning as well as classification method presented by Fix and Hodges, and it has proven itself to be an excellent recognition protocol. Decision rules perform excellently despite no explicit knowledge of the information available. Basic generalization of the technique is known as kNN rule, wherein novel patterns are sorted into classes with the most members present amongst kNN, may be utilized for obtaining excellent estimates of Bayes errors and probabilities of error asymptotically approach Bayes error [11].

If every instance in the dataset possesses n features that merge for forming n-dimensional vector:

$$X = (x_1, x_2, ..., x_n)$$

The n features are regarded as independent parameters.

All samples comprise another feature, represented by y (dependent parameter) whose value relies on other n features x. It is assumed that y is a categorical parameter while a scalar function f is present that designates class, y = f(x) for all such vectors.

The notion in kNN techniques is the identification of k instances in the training set whose non-dependent parameters x are like u, and to utilize the k instances for classifying the novel instance into class, v. If it is assumed that f is a smooth function, the notion is to search for instances in the training data close to t and then to calculate v from values of y for the instances.

Euclidean distance between points x as well as u is

$$d(x,u) = \sqrt{\sum_{i=1}^{n} (x_i - u_i)^2}$$

Other methods of measuring distance between points in the space of independent predictor parameters are examined. The most basic case is k=1 wherein it discovers instance in training set which is nearest to u and set v=y wherein y is the class of closest neighbouring instance.

2.7. J48 Classifier

J48 classifier is a basic C4.5 decision tree for classification. It generates binary trees. Decision tree method is helpful in the classification issue; trees are created for modeling the classification procedure. When tree is generated, it is employed on all tuples in the dataset and leads to classification of the tuple.

While creating a tree, J48 does not consider missing values that is, values for those items which may be estimated on the basis of what is known regarding the feature values for other records. The fundamental notion is the splitting of information into ranges on the basis of feature values for the items which are discovered in training instances. J48 permits classification through decision trees or rules created from them.

2.8. Neural Networks (NN) Classifier

Neural networks are computational models built up from basic processing units known as neurons and are typically structured in layers with complete or partial connections. The primary job of a neuron is the reception of activation values from neighbours, calculate outputs on the basis of weighted input variables and transmit outputs to neighbours [12].

Learning (training) in a network refers to the procedure of altering connection weights between neurons such that networks are capable of fulfilling particular tasks. Back Propagation is a popular learning protocol which is an iterative gradient decent protocol for minimizing error functions denoted by:

$$E = \frac{1}{2}\sum_{j=1}^{L}(d_j - o_j^M)^2$$

Wherein d_j as well as o_j denote expected output as well as current output of neuron j in the output layer correspondingly while L represents the quantity of neurons in the output layer. In the iterative technique, corrections to weight variables are calculated as well as appended to earlier values thus:

$$\begin{cases} \Delta w_{i,j} = -\eta \dfrac{\partial E}{\partial w_{i,j}} \\ \Delta w_{i,j}(t+1) = \Delta w_{i,j} + \alpha \Delta w_{i,j}(t) \end{cases}$$

Wherein $w_{i,j}$ refers to weight variable between neuron i as well as j. η refers to a positive constant which controls the quantity of adjustment and is known as learning rate, α refers to a momentum factor which is between 0 and 1 while "t" represents iteration count. Variable α smoothens fast modifications between weights. Learning rate as well as momentum variable has great influence on the learning process's success.

3. Experimental Results

In this section, number of images used: 85 normal and 35 sarcoma. The CFS and PSO feature selection based KNN, J48 and NN classifiers are evaluated. The classification accuracy, average positive predictive value, average sensitivity and average f measure are shown in figure 5 to 8. The sample image 1 & 2 are illustrated in figure 3 & 4.

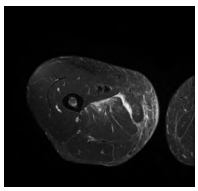
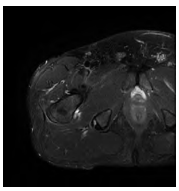
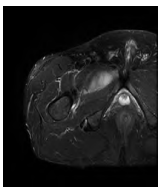

(a) (b) (c)

Fig.3 Sample Images MRI (a, b & c)

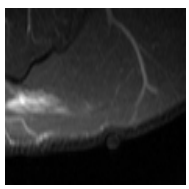
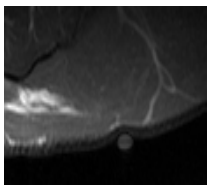
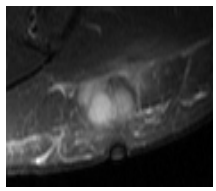

(d) (e) (f)

Fig.4 Sample Images FDG-PET (d, e & f)

Table 2.*CFS and PSO Feature Selection based KNN, J48 & NN Classifiers*

	CFS-KNN	CFS-J48	CFS-NN	PSO-KNN	PSO-J48	PSO-NN
Classification Accuracy	0.8167	0.8417	0.875	0.85	0.8667	0.8966
Positive Predictive Value for Normal	0.6512	0.6905	0.7632	0.7179	0.7568	0.8
Positive Predictive Value for Bone Sarcoma	0.9091	0.9231	0.9268	0.9136	0.9157	0.9383
Sensitivity for Normal	0.8	0.8286	0.8286	0.8	0.8	0.8485
Sensitivity for Bone Sarcoma	0.8235	0.8471	0.8941	0.8706	0.8941	0.9157
F measure for Normal	0.8642	0.8835	0.9102	0.8916	0.9048	0.9269
F measure for Bone Sarcoma	0.718	0.7533	0.7946	0.7567	0.7778	0.8235

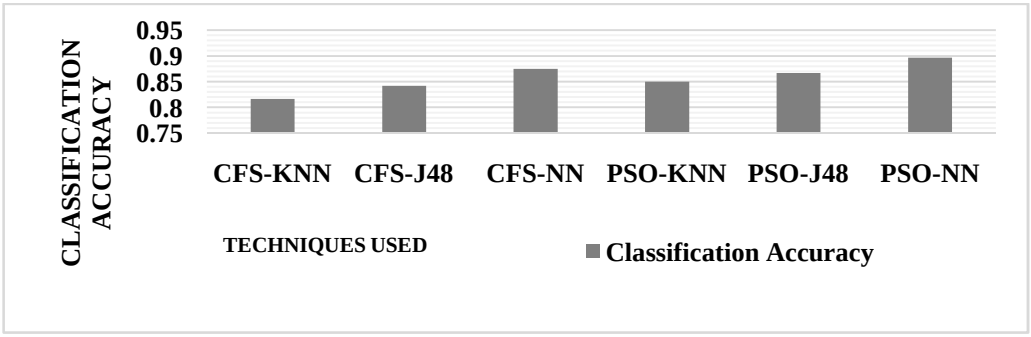

Fig. 5 Classification Accuracy

From the figure 5, it can be observed that the PSO-NN has higher classification accuracy by 9.32% compared for CFS-KNN, by 6.31% for CFS-J48, by 2.43% for CFS-NN, by 5.33% for PSO-KNN and 3.39% for PSO-J48.

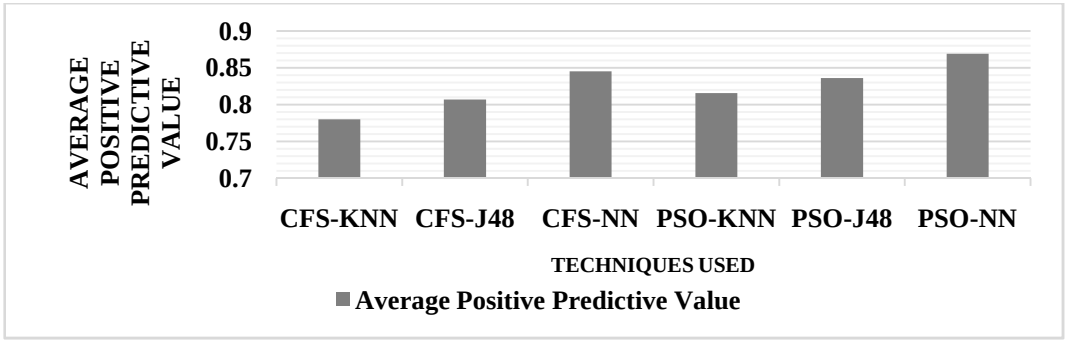

Fig. 6 Average Positive Predictive Value

From the figure 6, it can be observed that the PSO-NN has higher average positive predictive value by 10.79% compared for CFS-KNN, by 7.44% for CFS-J48, by 2.81% for CFS-NN, by 6.33% for PSO-KNN and 3.85% for PSO-J48.

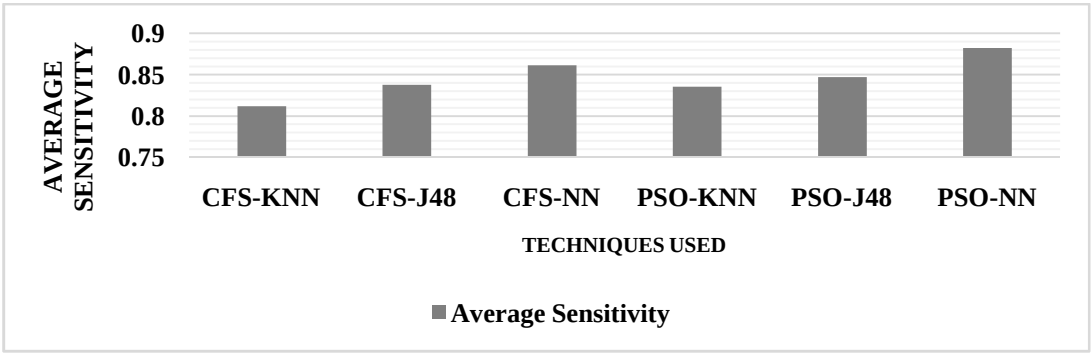

Fig. 7 Average Sensitivity

From the figure 7, it can be observed that the PSO-NN has higher average sensitivity by 8.3% compared for CFS-KNN, by 5.14% for CFS-J48, by 2.38% for CFS-NN, by 5.45% for PSO-KNN and 4.05% for PSO-J48.

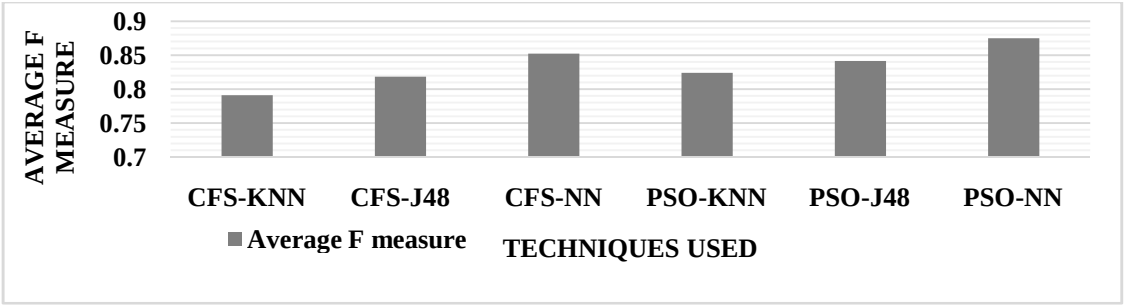

Fig. 8 Average F Measure

From the figure 8, it is observed that PSO-NN has higher average f measure by 10.09% compared for CFS-KNN, by 6.7% for CFS-J48, by 2.63% for CFS-NN, by 6% for PSO-KNN and 3.94% for PSO-J48.

4. Conclusion

In the current study, a new method on the basis of combination of FDG-PET as well as MRI volumes for improvement assessments of histological responses in bone sarcoma afflicted individuals is studied. Innovative feature extraction & feature selection techniques and various classifiers were also developed.Results show that the PSO-NN has higher classification accuracy by 9.32% compared for CFS-KNN, by 6.31% for CFS-J48, by 2.43% for CFS-NN, by 5.33% for PSO-KNN and 3.39% for PSO-J48.

References

[1] Honoré, C., Méeus, P., Stoeckle, E., &Bonvalot, S. (2015). Soft tissue sarcoma in France in 2015: Epidemiology, classification and organization of clinical care. Journal of visceral surgery, 152(4), 223-230..

[2] Maheshwari, A. V., & Cheng, E. Y. (2010). Ewing sarcoma family of tumors. Journal of the American Academy of Orthopaedic Surgeons, 18(2), 94-107.

[3] Denecke, T., Hundsdörfer, P., Misch, D., Steffen, I. G., Schönberger, S., Furth, C., ...& Kluge, R. (2010). Assessment of histological response of paediatric bone sarcomas using FDG PET in comparison to morphological volume measurement and standardized MRI parameters. European journal of nuclear medicine and molecular imaging, 37(10), 1842-1853.

[4] Tateishi, U., Yamaguchi, U., Seki, K., Terauchi, T., Arai, Y., & Kim, E. E. (2007). Bone and Soft-Tissue Sarcoma: Preoperative Staging with Fluorine 18 FluorodeoxyglucosePET/CT and Conventional Imaging 1. Radiology, 245(3), 839-847.

[5] Singh, L., &Chetty, G. (2012, December). A comparative study of MRI data using various machine learning and pattern recognition algorithms to detect brain abnormalities. In Proceedings of the Tenth Australasian Data Mining Conference-Volume 134 (pp. 157-165). Australian Computer Society, Inc..

[6] Freeman, C. R., Skamene, S. R., & El Naqa, I. (2015). A radiomics model from joint FDG-PET and MRI texture features for the prediction of lung metastases in soft-tissue sarcomas of the extremities. Physics in medicine and biology, 60(14), 5471.

[7] Vinoth, M., &Jayalakshmi, B. (2014). Bone Mineral Density Estimation Using Digital X-Ray Images For Detection Of Rheumatoid Arthritis. International Journal of Pharma and Bio Sciences, 5 (3) : (B) 104 - 121.

[8] Kharat, K. D., Kulkarni, P. P., &Nagori, M. B. (2012). Brain tumor classification using neural network based methods. International Journal of Computer Science and Informatics, 1(4).

[9] Zhang, Y., Dong, Z., Wu, L., & Wang, S. (2011). A hybrid method for MRI brain image classification. Expert Systems with Applications, 38(8), 10049-10053.

[10] Kaur, A., & Singh, M. D. (2012). An overview of pso-based approaches in image segmentation. Int J EngTechnol, 2(8), 1349-1357.

[11] Patil, T. R., &Sherekar, S. S. (2013). Performance analysis of Naive Bayes and J48 classification algorithm for data classification. International Journal of Computer Science and Applications, 6(2), 256-261.

[12] Ahmadia, F. F., Zoeja, M. V., Ebadia, H., &Mokhtarzadea, M. (2008). The Application Of Neural Networks, Image Processing And CAD-Based Environments Facilities In Automatic Road Extraction And Vectorization From High Resolution Satellite Images. The International Archives of the Photogrammetry, Remote Sensing and Spatial Information Sciences, 37, 585-592.